

Supporting Information

Highly conductive nanostructured PEDOT polymer confined into the mesoporous MIL-100(Fe)

Pablo Salcedo-Abraira,^{a†} Andrea Santiago-Portillo,^{b†} Pedro Atienzar,^b Pierre Bordet,^c Fabrice Salles,^d Nathalie Guillou,^e Erik Elkaim,^f Hermenegildo García,^b Sergio Navalón,^{b,*} Patricia Horcajada^{a,*}

^aAdvanced Porous Materials Unit, IMDEA Energy, Avda. Ramón y Cajal 3, 28935 Móstoles-Madrid, Spain

^bDepartment of Chemistry and Instituto de Tecnología Química, Consejo Superior de Investigaciones Científicas-Universitat Politècnica de València, Universitat Politècnica de València, C/Camino de Vera, s/n, 46022, Valencia, Spain

^cInstitute NEEL CNRS/UGA, 25 rue des Martyrs, Grenoble cedex 9, France.

^dInstitut Charles Gerhardt Montpellier, UMR 5253 CNRS UM ENSCM, Université Montpellier, Place E. Bataillon, 34095 Montpellier Cedex 05, France

^eInstitut Lavoisier de Versailles, UMR CNRS 8180, Université de Versailles St-Quentin en Yvelines, Université Paris Saclay, 45 Av. des Etats-Unis, 78035 Versailles, France

^fCRISTAL Beamline, Synchrotron Soleil, L'orme des Merisiers, Saint-Aubin, BP 48, 91192 Gif-sur-Yvette Cedex, France

[†]These authors contributed to this manuscript equally

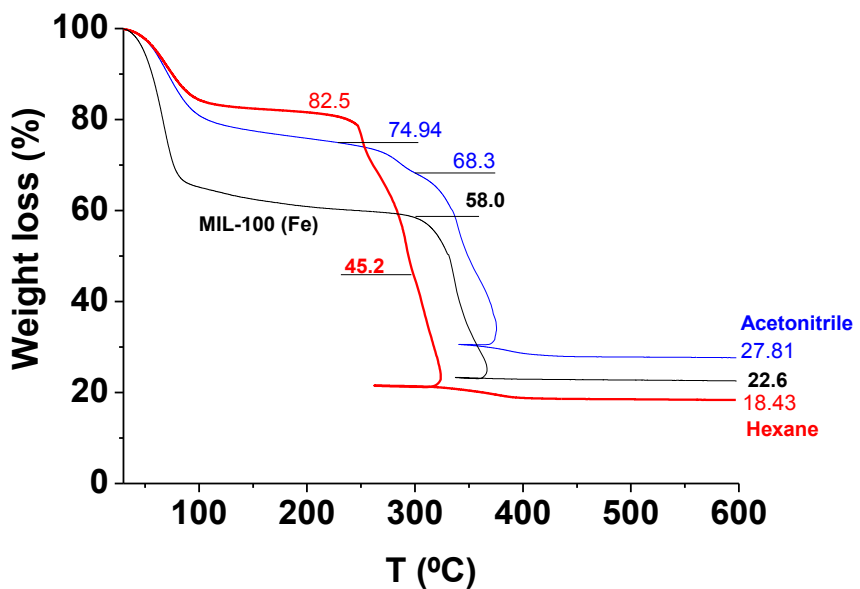


Figure S1.TGA curves of PEDOT@MIL-100(Fe) encapsulated in acetonitrile (blue) or hexane (red), together with the empty MIL-100(Fe) solid (black)

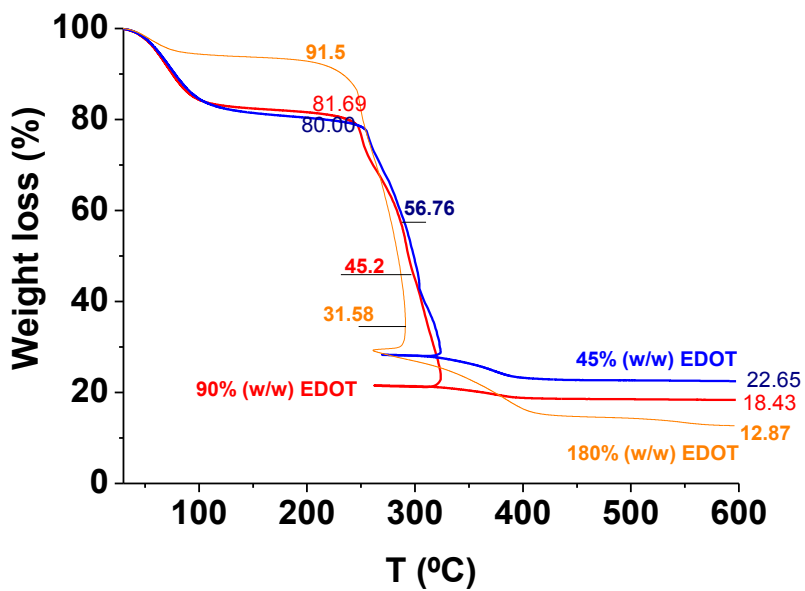


Figure S2. TGA curves of PEDOT@MIL-100 (Fe)-1 (blue), 2 (red) and 3 (orange) composites

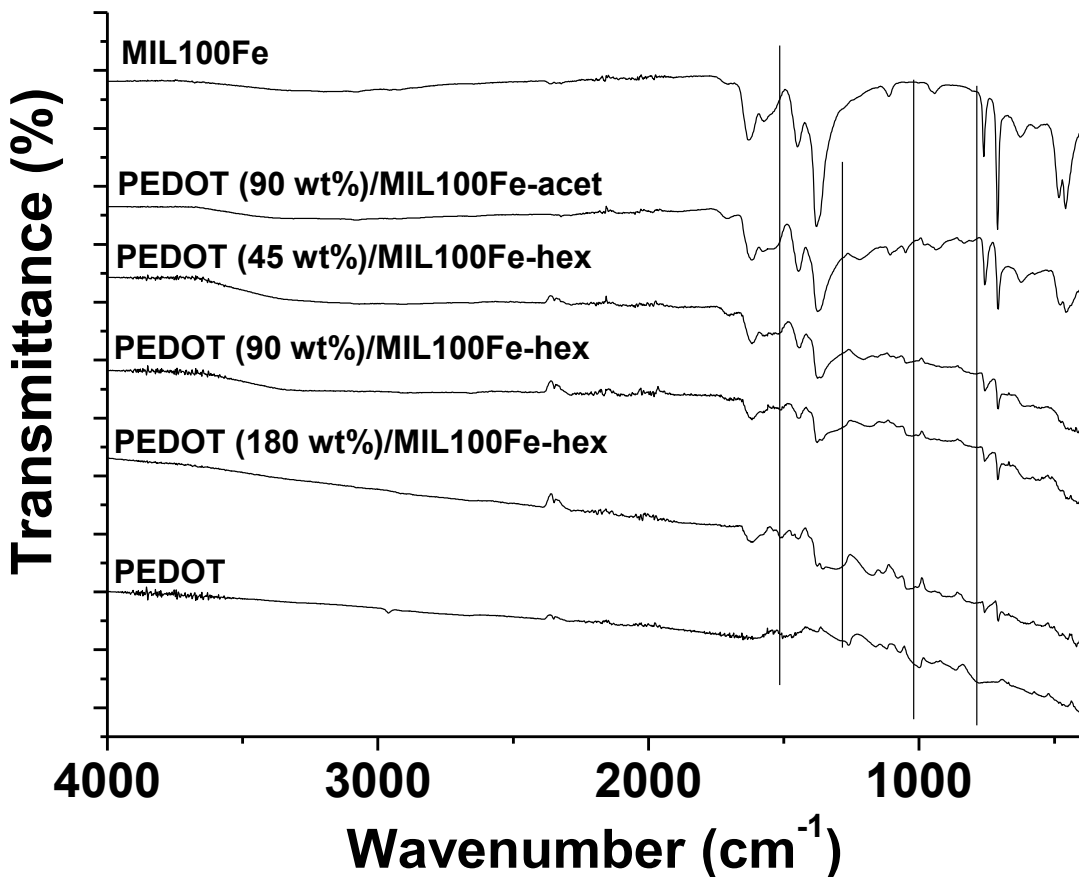


Figure S3. FTIR spectra of MIL-100(Fe) (a), PEDOT-MIL100(Fe)-1 (b), PEDOT-MIL100(Fe)-2 (c), PEDOT-MIL100(Fe)-3 (d) and as-prepared PEDOT (c).

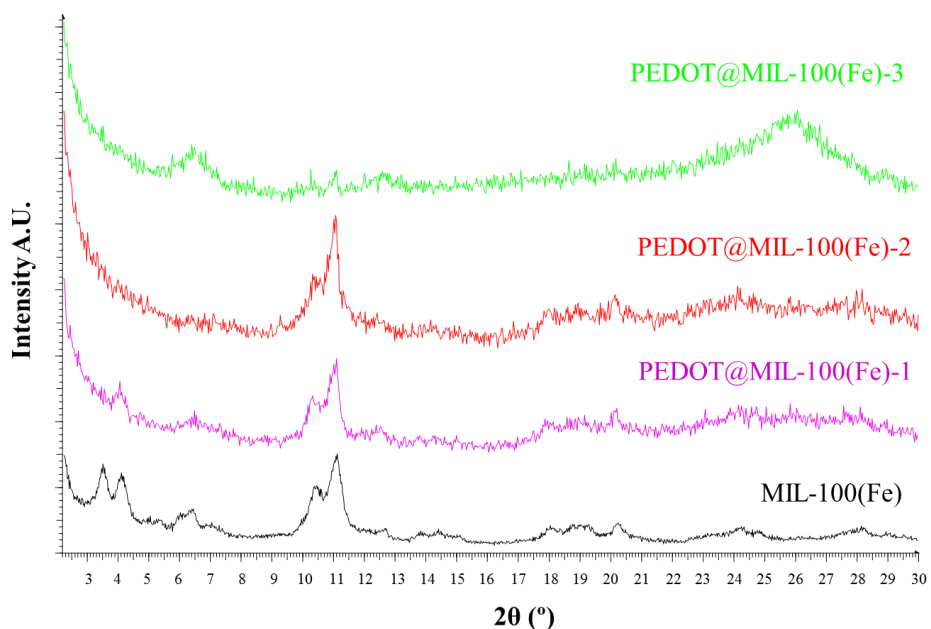


Figure S4. PXRD patterns of MIL-100(Fe) (Black) and PEDOT@MIL-100(Fe)-1 (pink), 2 (red) and-3 (green) composites.

Table S1. Elemental composition of free PEDOT and amount of PEDOT inside the MIL-100(Fe)-2

	Theo. vs exp.
Free PEDOT Fe/S at. ratio	0 vs $0,08 \pm 0,05$
Free PEDOT Cl/S at. ratio	$0,3 \pm 0,33 \pm 0,12$
PEDOT@MIL-100(Fe)-2.	
PEDOT (%wt; dry empty solid)	60 ± 9
Number of EDOT monomer/u.c.	1062 ± 174
Number EDOT monomer/large cage	58 ± 9
Number EDOT monomer/small cage	37 ± 6
<hr/>	
Number total Cl/u.c.	1365 ± 363
Cl/S at. Ratio	1.28 ± 0.33
Considering 1 Cl⁻ / 3 EDOT	354 ± 58
Number excess Cl/u.c.	1011 ± 319
Number Fe total/u.c.	2003 ± 581
Number Fe MIL100/u.c.	1152
Number Fe excess/u.c.	851 ± 581
Excess Fe/Fe MIL100 (u.c.)	$0,74 \pm 0,50$

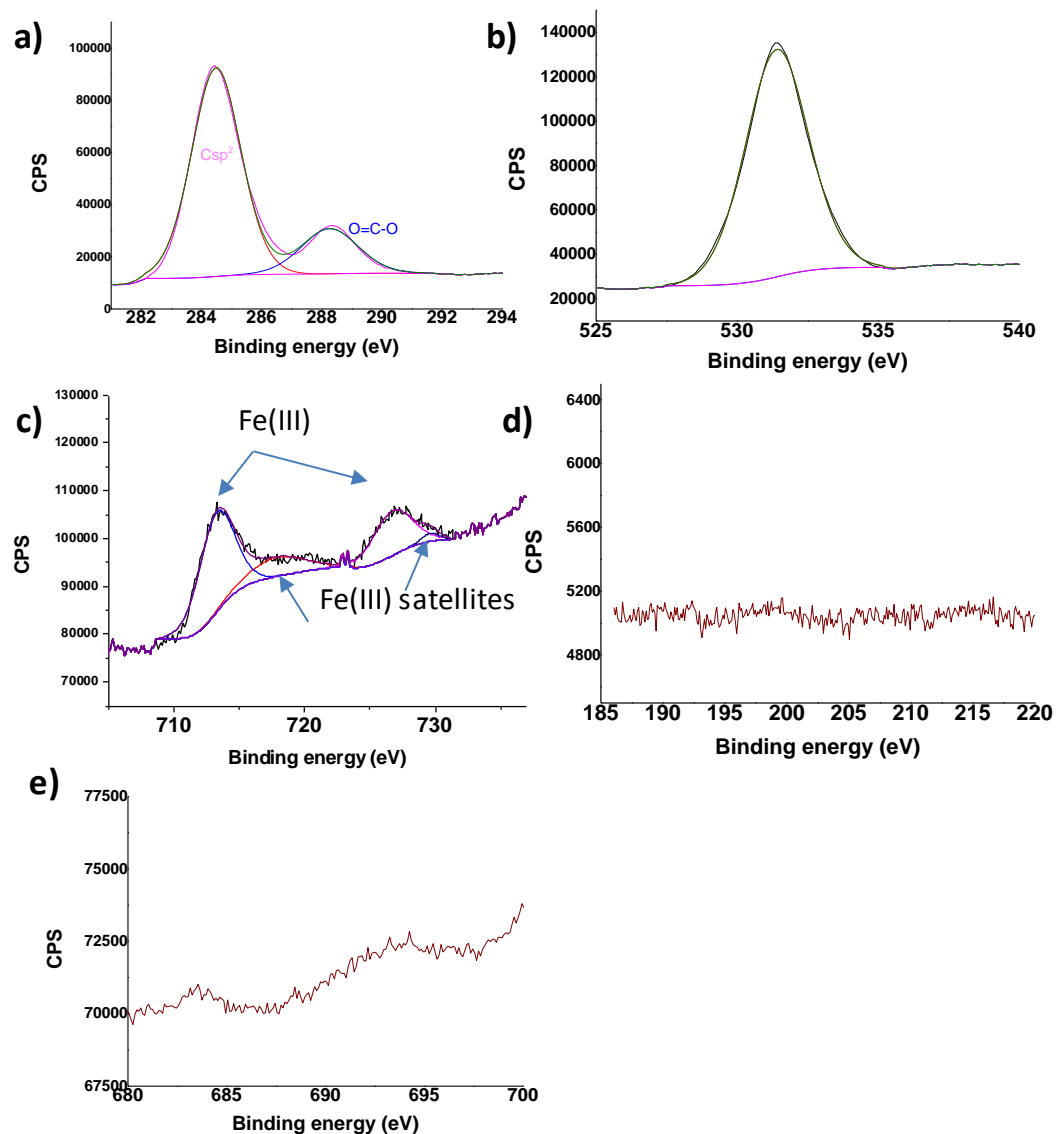


Figure S5. XPS of MIL-100(Fe). Legend: (a) C 1s; (b) O 1s; (c) Fe 2p; (d) Cl 2p; (e) F 1s.

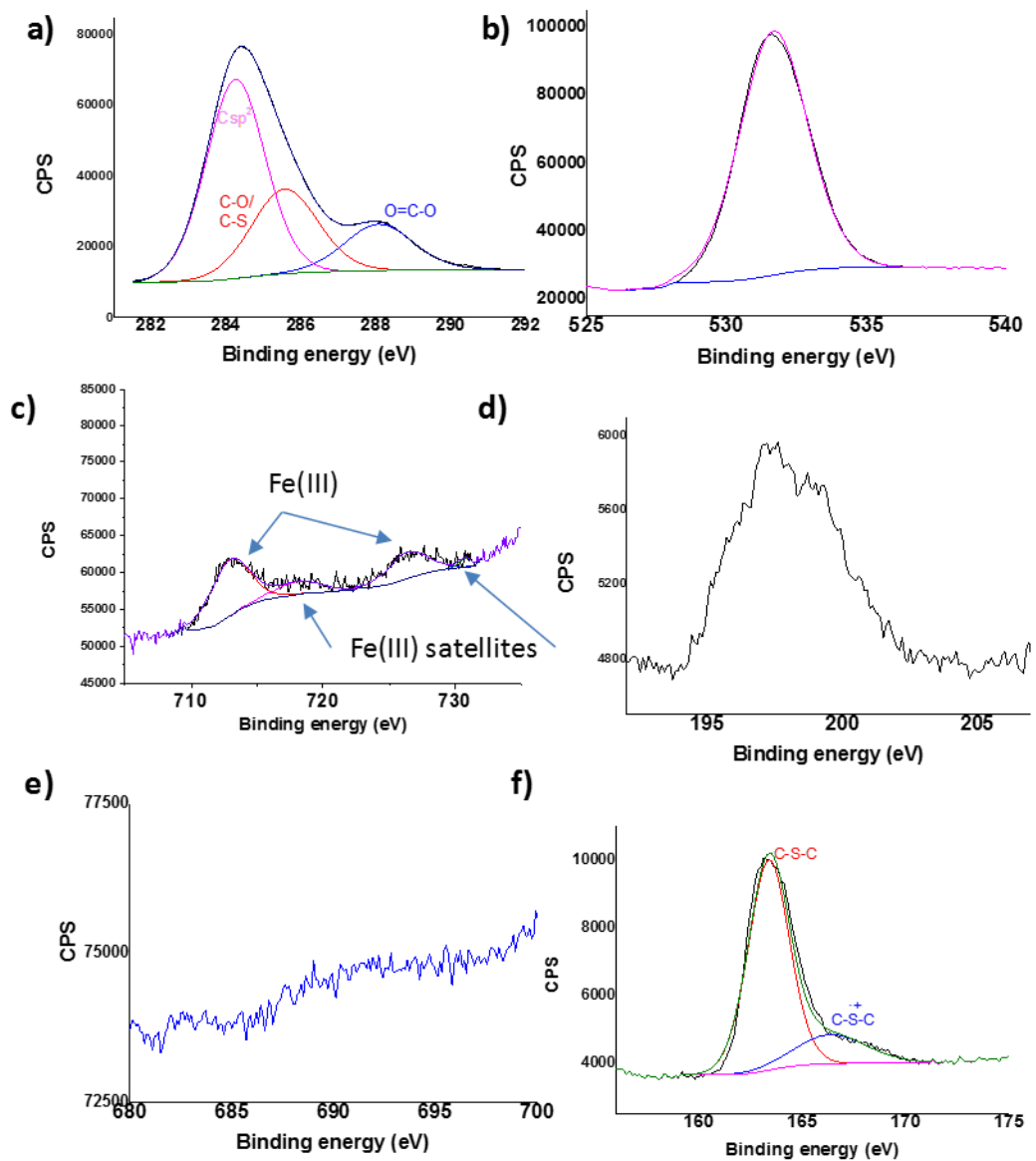


Figure S6. XPS of PEDOT@MIL-100(Fe)-2. Legend: (a) C 1s; (b) O 1s; (c) Fe 2p; (d) Cl 2p; (e) F 1s; (f) S 2p

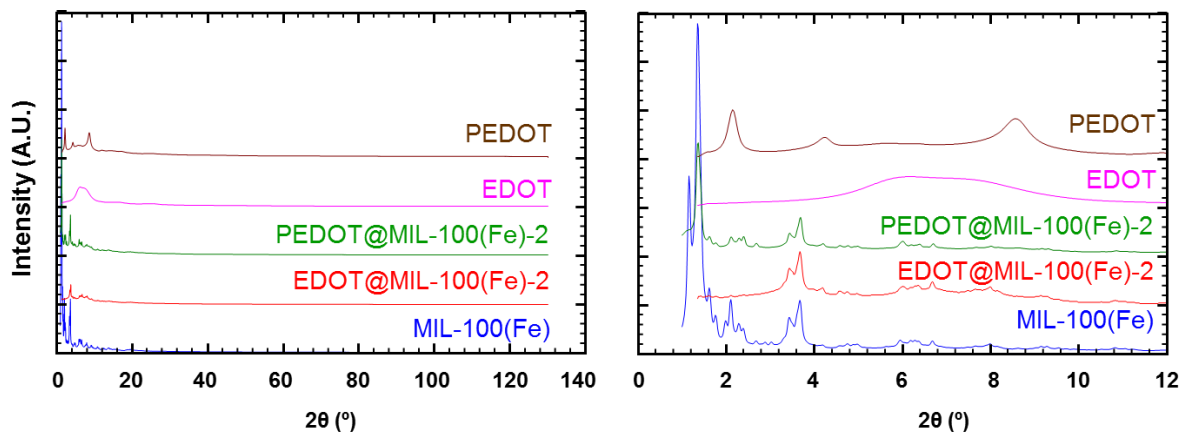


Figure S7. PXRD patterns collected by using synchrotron radiation

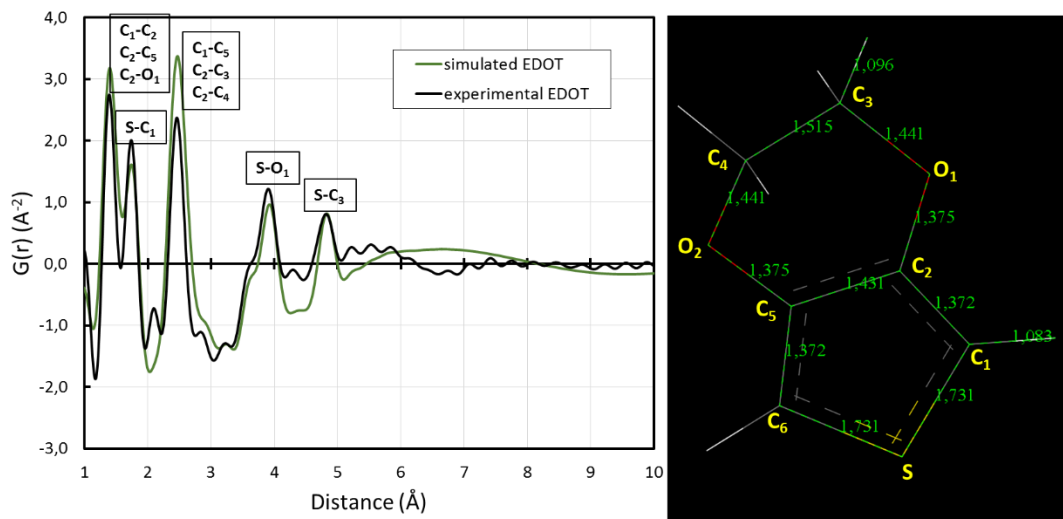


Figure S8. Left: Simulated and experimental PDF analysis of EDOT molecule. Right: DFT Simulated chemical structure of isolated EDOT together with the main atomic distances.

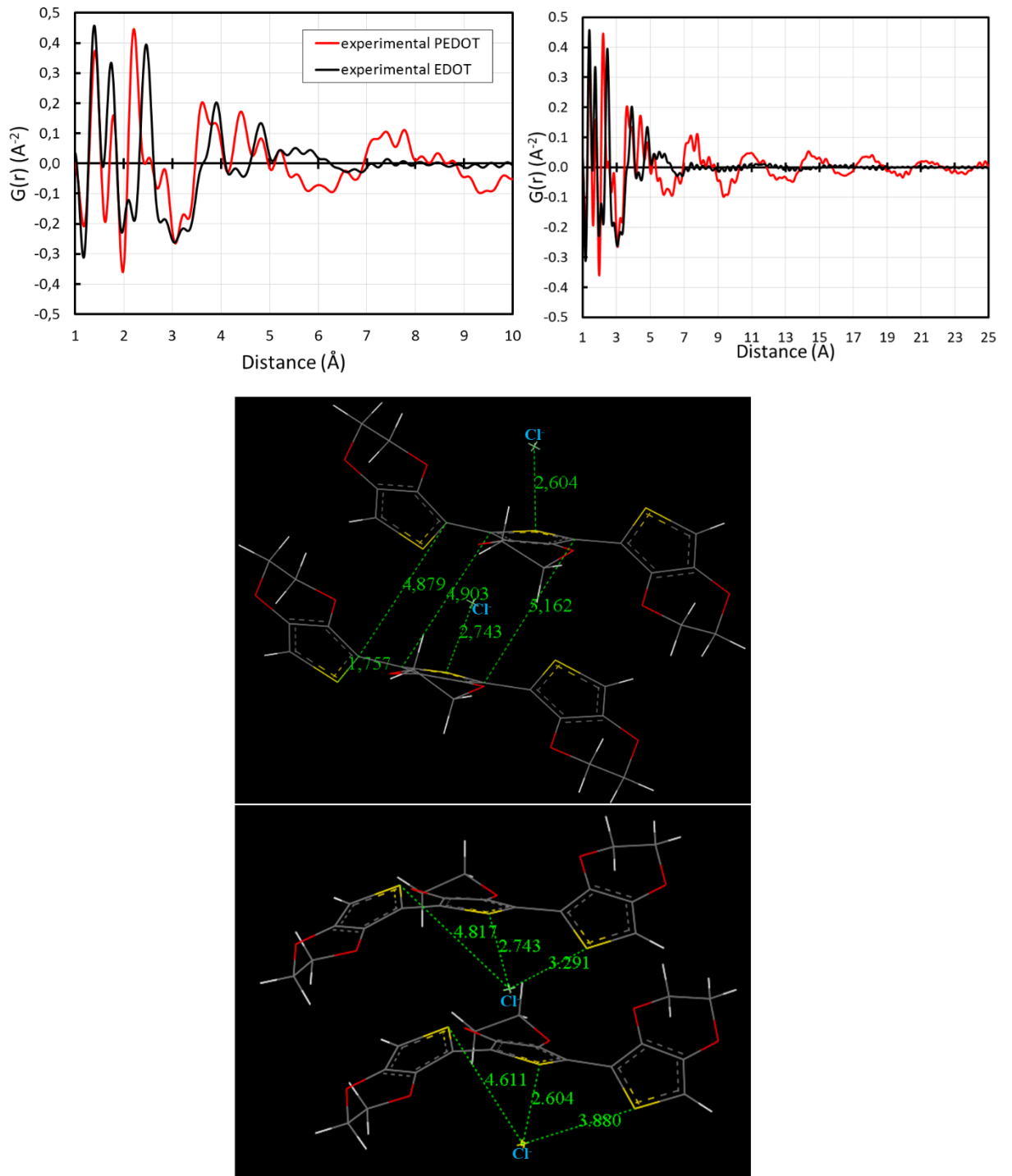


Figure S9. Top: experimental PDFs of EDOT and PEDOT up to 10 (left) and 25 Å (right). Bottom: DFT simulated chemical structure of free PEDOT together with the main atomic distances. Sulphur, carbon, oxygen, hydrogen and chlorine are in yellow, grey, red, white and blue respectively.

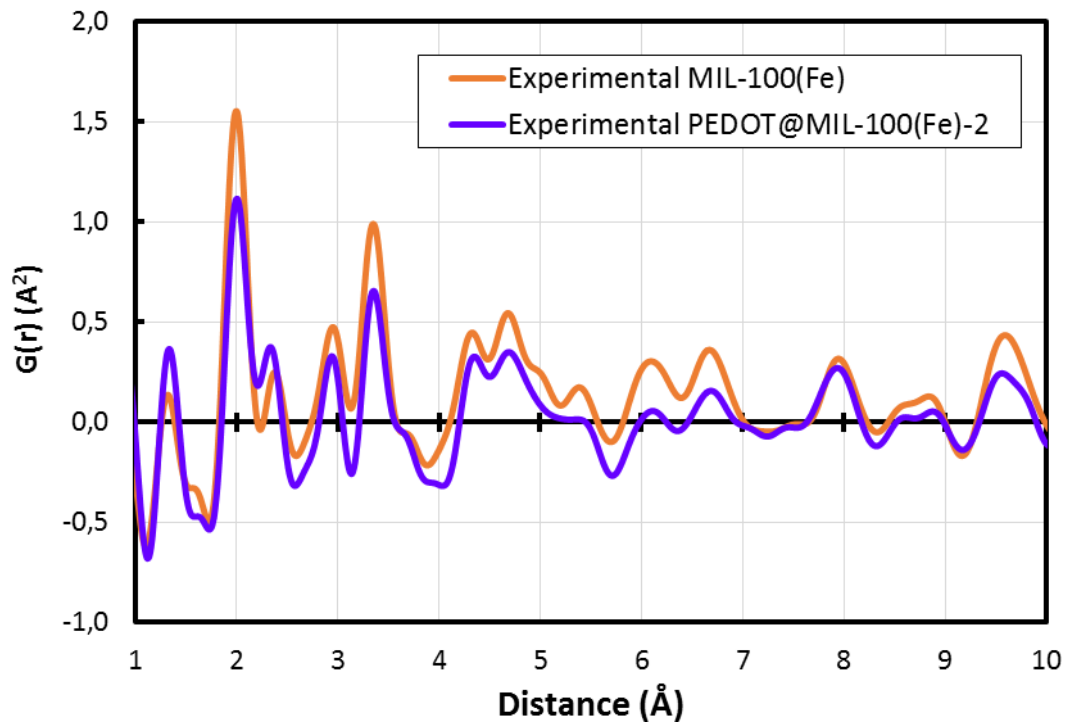


Figure S10. Comparison of the PDFs of MIL-100(Fe) and PEDOT@MIL-100(Fe).

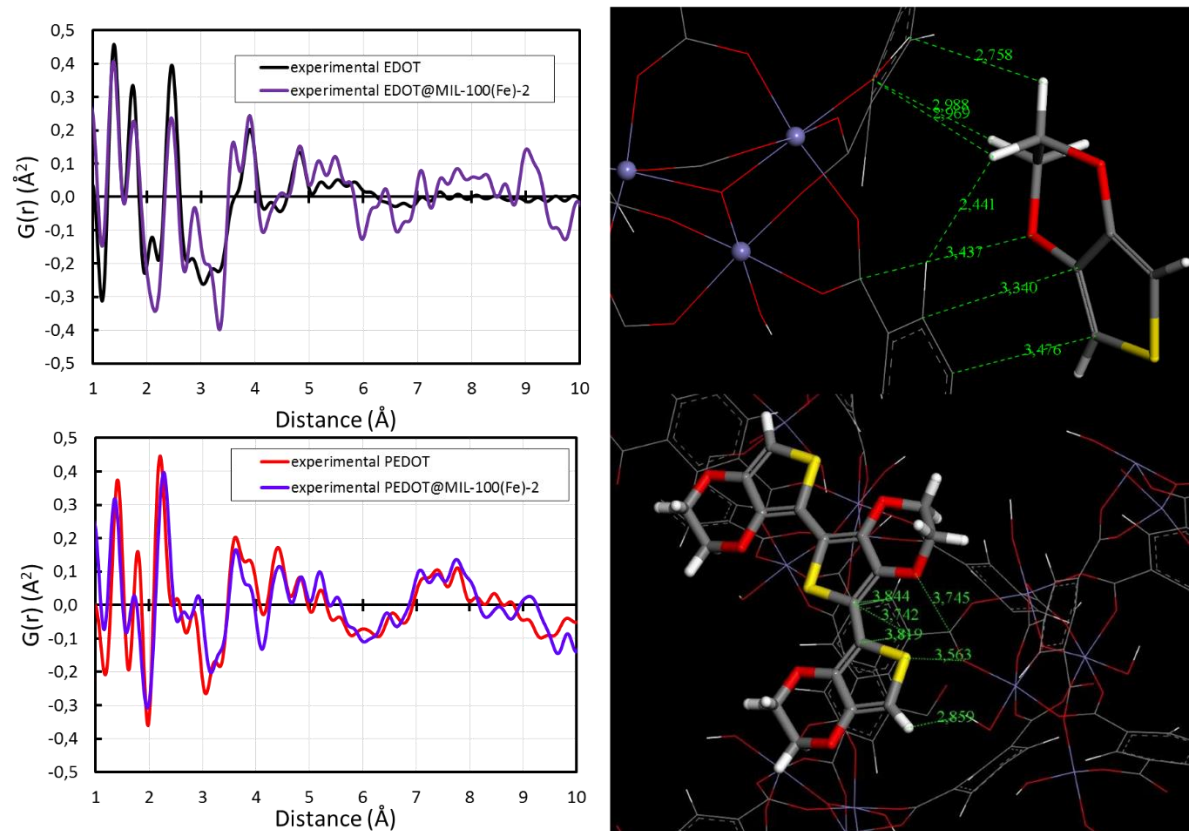


Figure S11. Top: Subtracted PDF contribution of the EDOT in the EDOT@MIL-100(Fe) compared with the free EDOT. Bottom: Subtracted PDF contribution of the PEDOT in the PEDOT@MIL-100(Fe)-2 compared with the free PEDOT. Sulphur, carbon, oxygen, hydrogen and iron are in yellow, grey, red, white and purple respectively

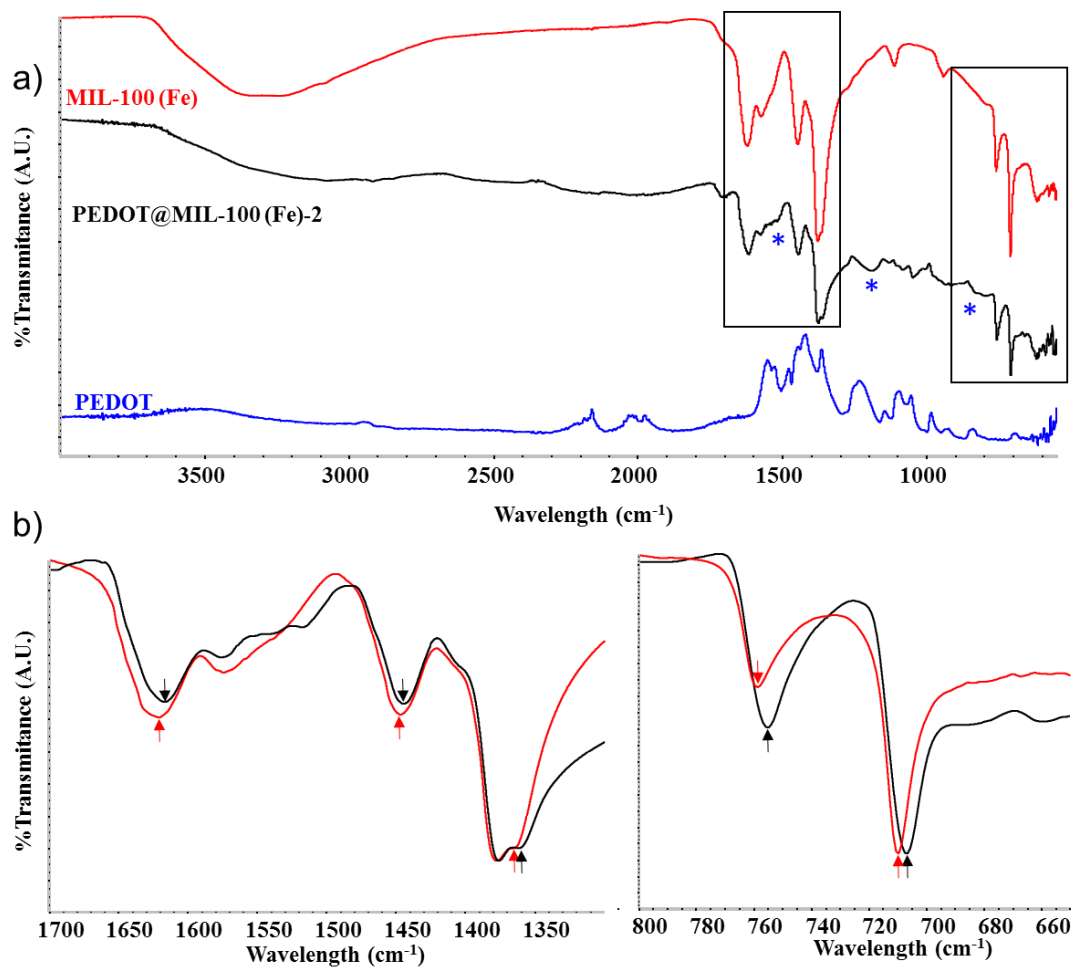


Figure S12. a) FTIR spectra of MIL-100(Fe) (red), PEDOT@MIL-100(Fe)-2 (black) and isolated PEDOT (blue) (Asterisk indicate the presence of PEDOT bands in PEDOT@MIL-100(Fe)) and b) zoom of the selected areas.

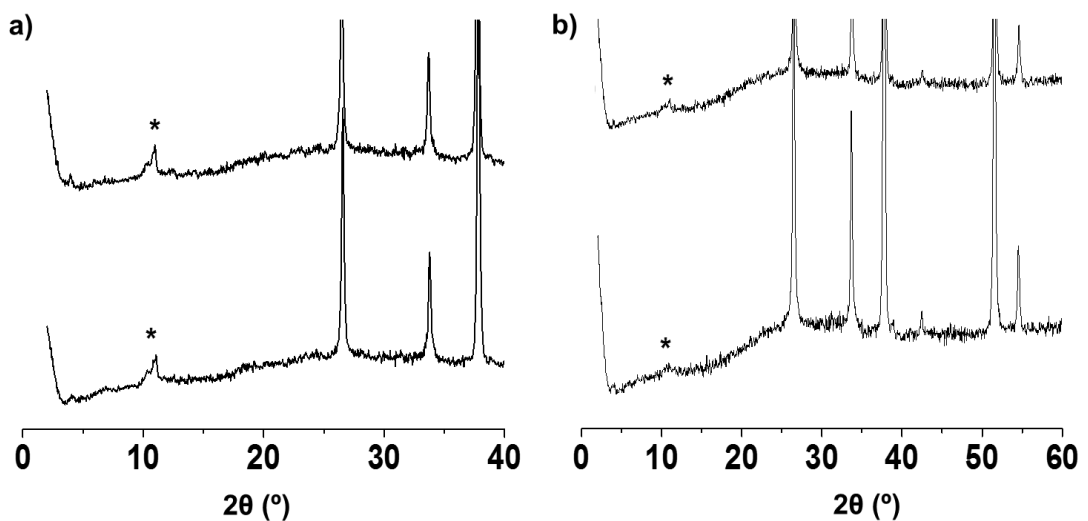


Figure S13. XRD patterns of: a) PEDOT@MIL-100(Fe)-2 thin film on FTO before (bottom) and after (up) of 50 cycles of cyclic voltammetry and b) PEDOT@MIL-100(Fe)-2 thin film on FTO before (bottom) and after (up) of 20 cycles of electrochromic switching. Asterisk indicate diffraction peaks corresponding to the MIL-100(Fe) material.

Cyclic voltammetry Electrochromic switching

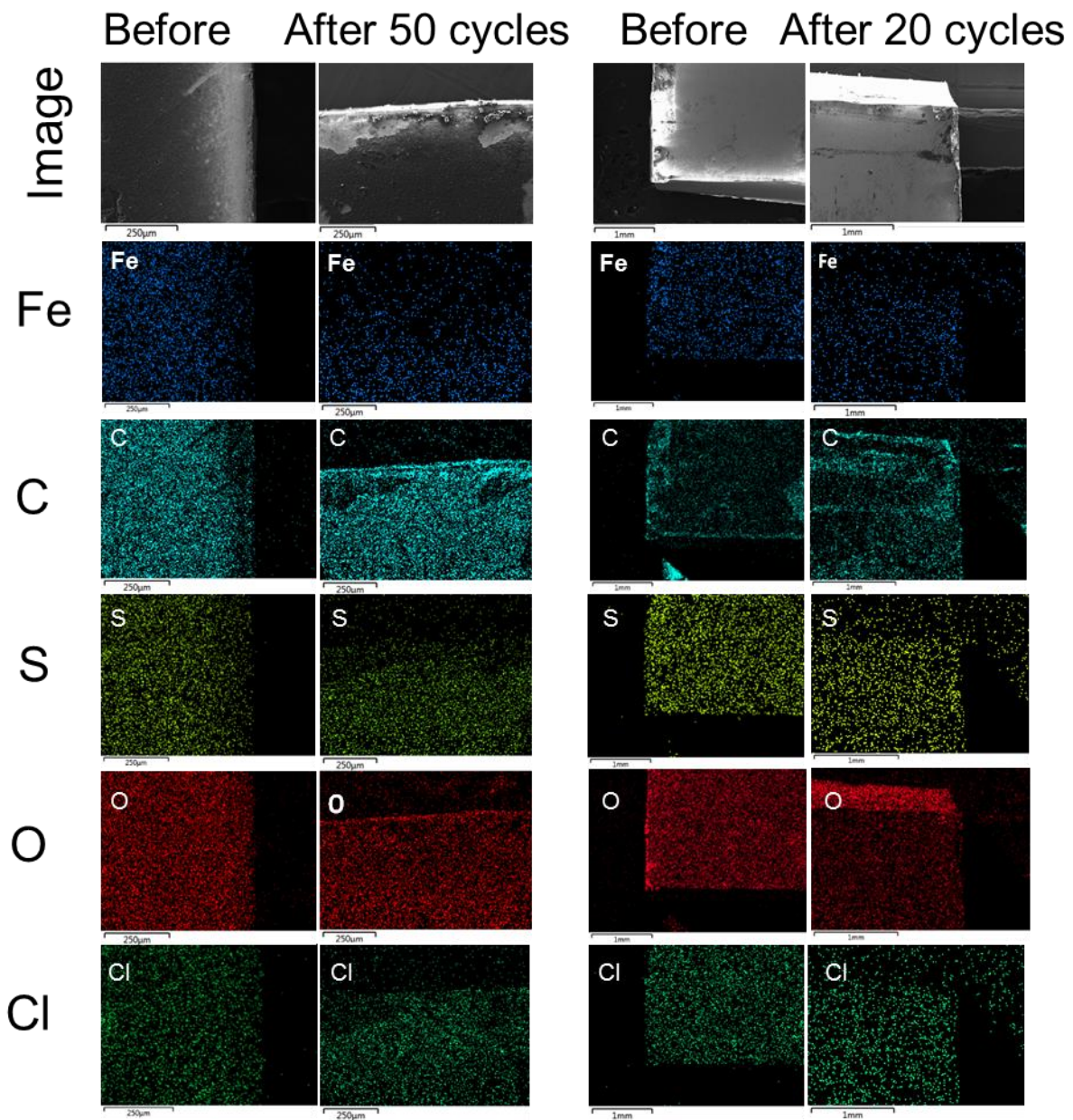


Figure S14 SEM-EDX analysis of the PEDOT-MIL-100(Fe)-2 flat surface supported on FTO employed for cyclic voltammetry measurements (left) and for electrochromism measurements (right).

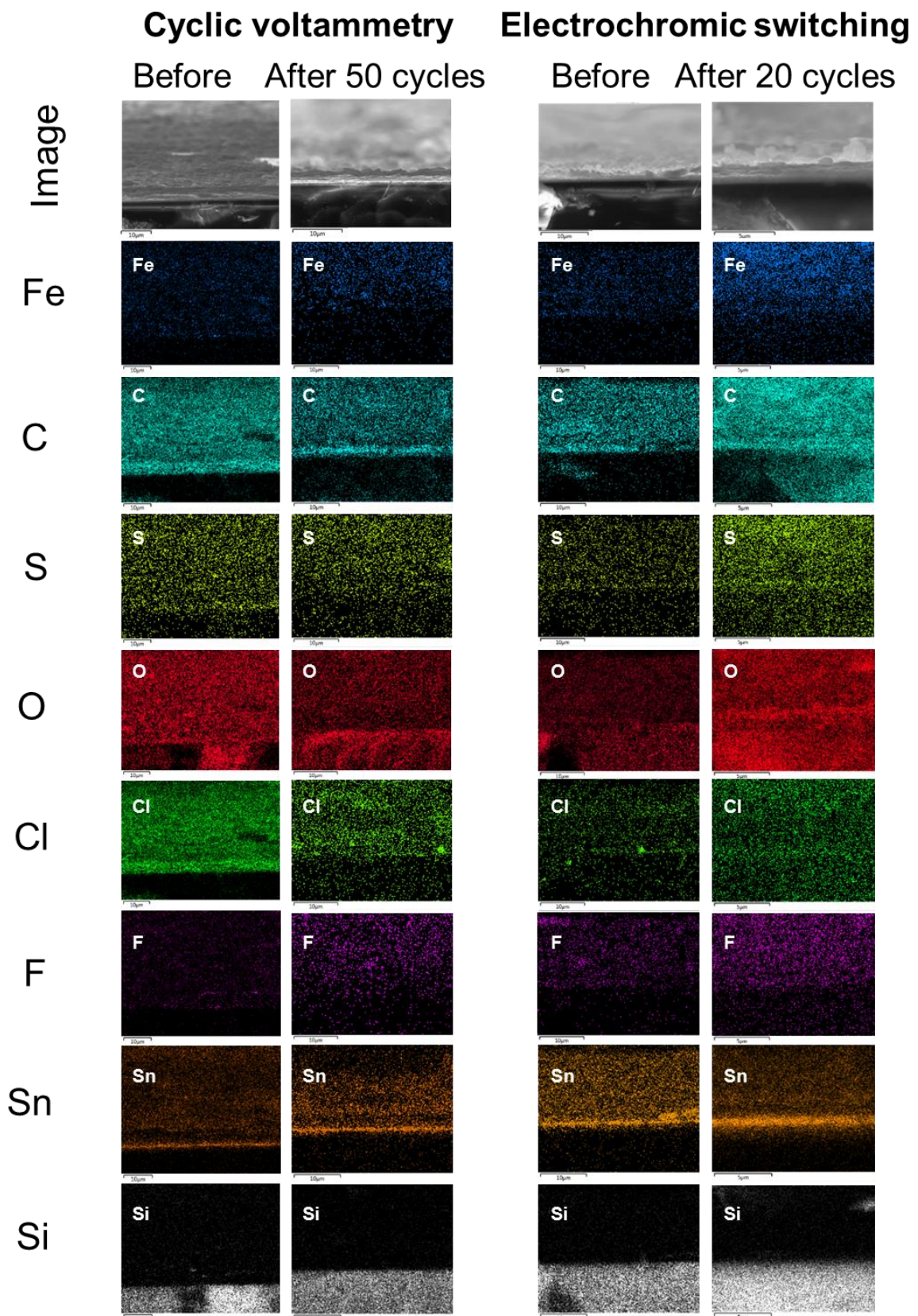


Figure S15. SEM-EDX analysis of the PEDOT-MIL-100(Fe)-2 film thickness supported on FTO employed for cyclic voltammetry measurements (left) and for electrochromism measurements (right)

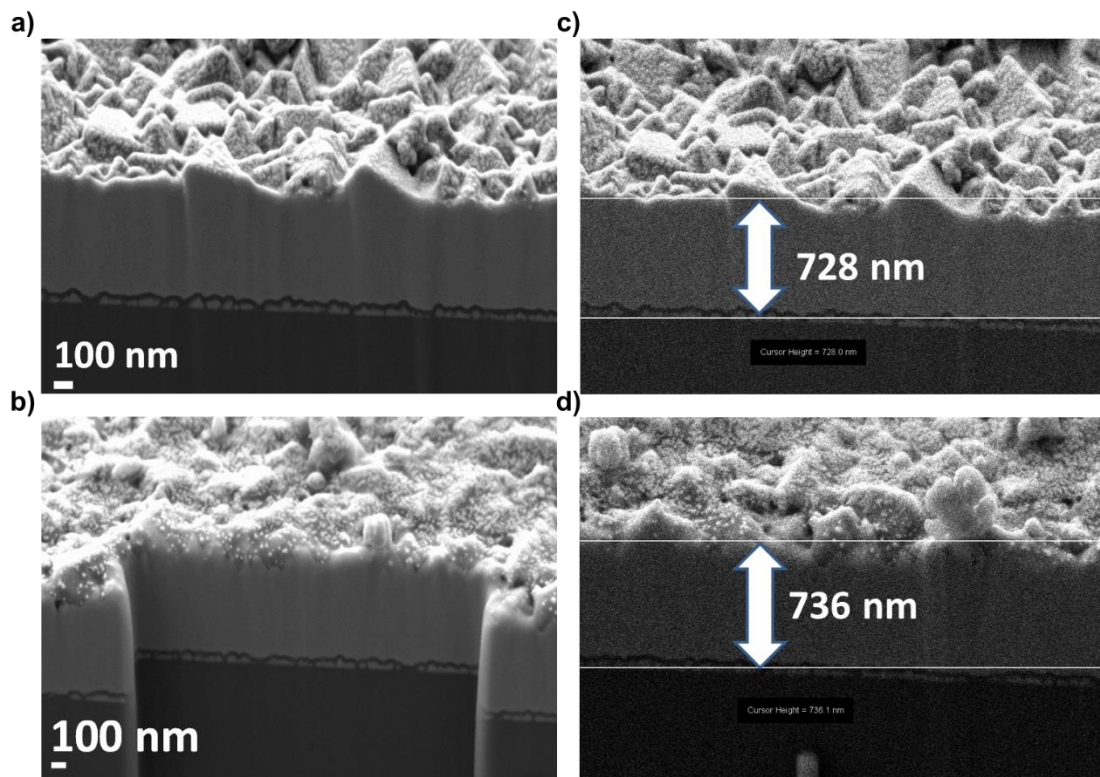


Figure S16. FIB-SEM images of: (a) the fresh PEDOT@MIL-100(Fe)-2 film; (b) the used PEDOT@MIL-101(Fe)-2 sample after 50 cycles of voltammetry; PEDOT@MIL-100(Fe)-2 before (c) and after (d) used in the 50 cycles of the cyclic voltammetry. Note: fast SEM images were recorded (c,d) with low quality on purpose to properly measure the thickness minimizing possible error due to the movement of the sample.

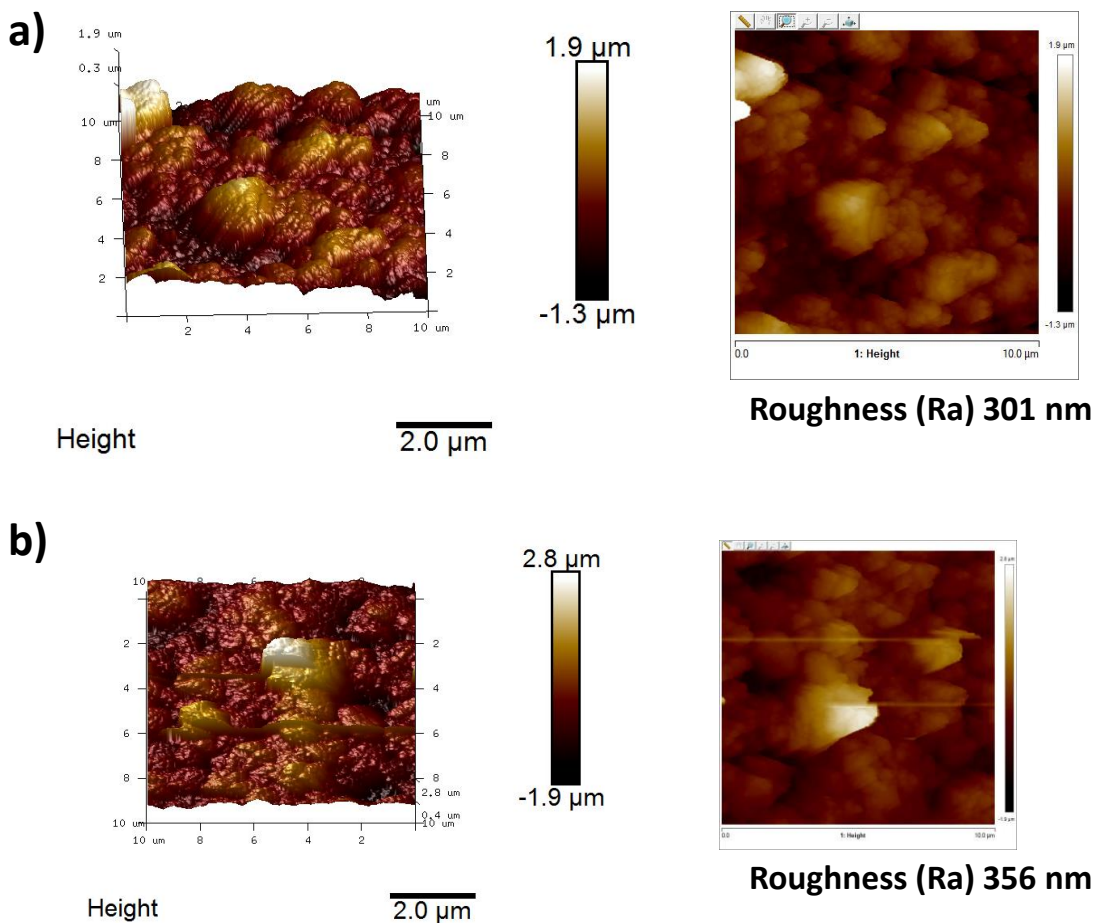


Figure S17. AFM images of PEDOT@MIL-100(Fe)-2 film before (a) and after (b) 50 cyclic voltammetry cycles and roughness estimation.

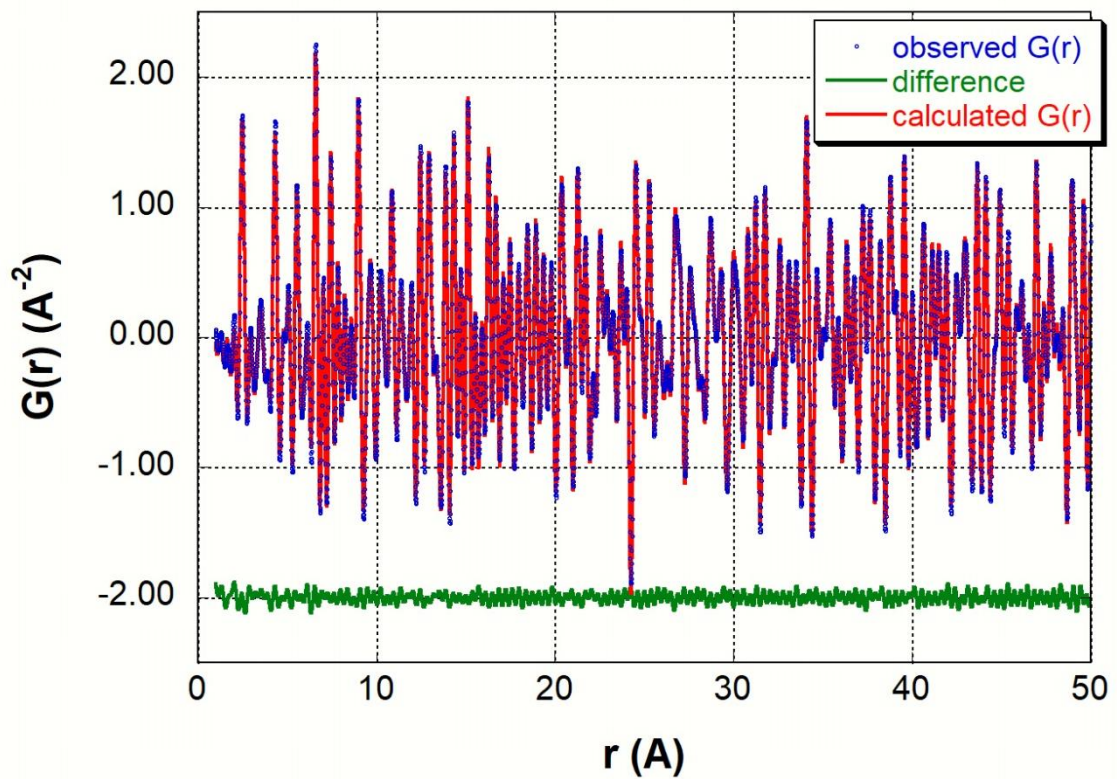


Figure S18: Result of the fit of the PDF from the Ni standard sample.

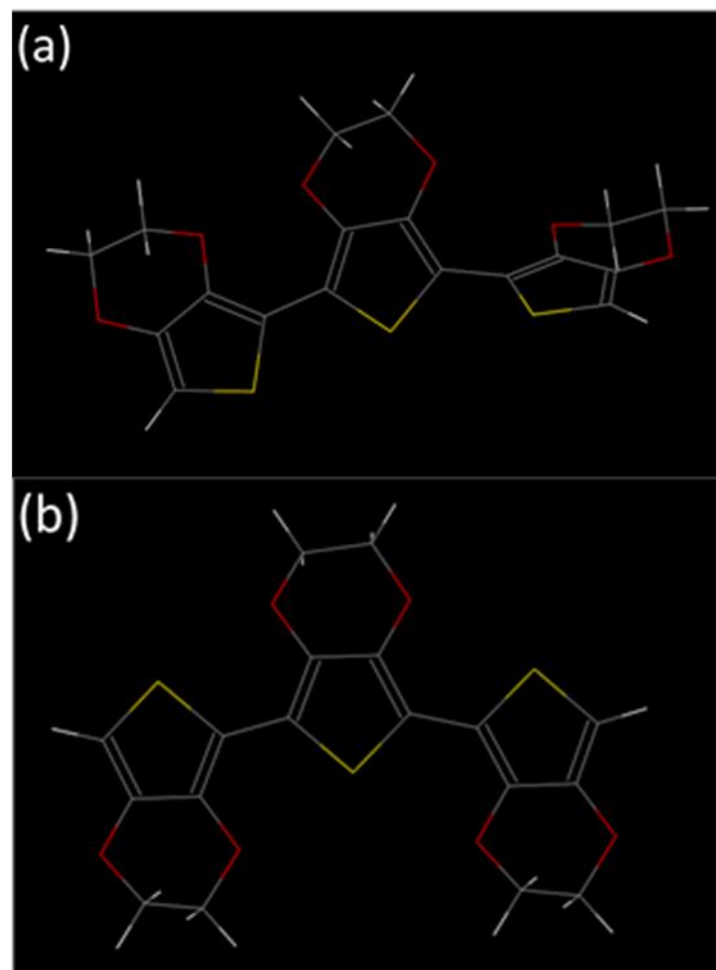


Figure S19: Conformations of the PEDOT investigated by DFT calculations

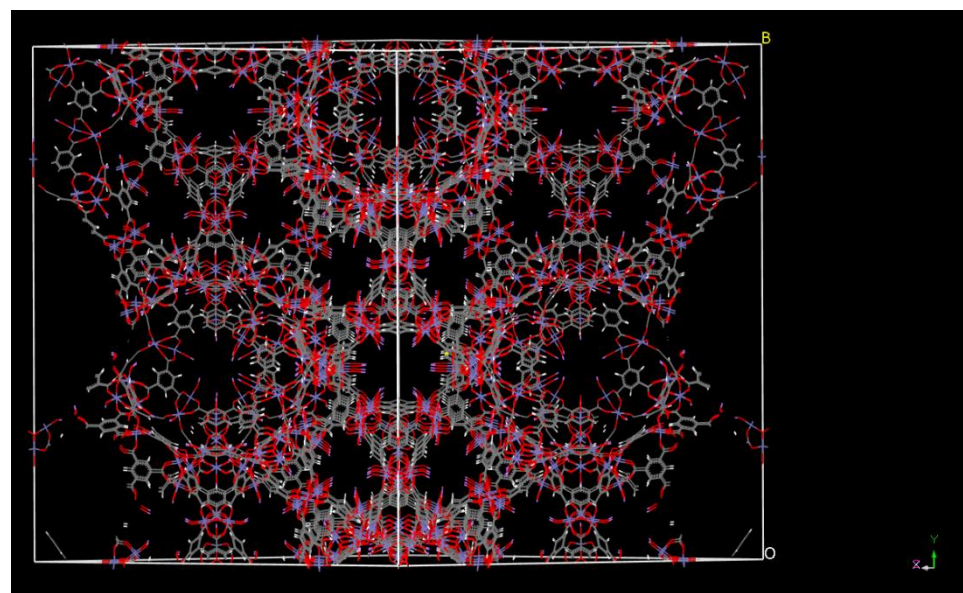


Figure S20: Model of MIL-100 from literature (Horcajada et al., Chem. Commun., 2007, 2820-2822)